International Journal of Thermal Sciences 48 (2009) 1398–1404

Contents lists available at ScienceDirect

International Journal of Thermal Sciences

www.elsevier.com/locate/ijts

Inverse problem of estimating space and time dependent hot surface heat flux in transient transpiration cooling process

Junxiang Shi *, Jianhua Wang

Department of Thermal Science and Energy Engineering, University of Science and Technology of China, Jinzhai Road No. 96, Hefei, 230027 Anhui, PR China

ARTICLE INFO

Article history:
Received 25 August 2008
Received in revised form 21 November 2008
Accepted 24 November 2008
Available online 16 December 2008

Keywords:
Inverse problem
Transpiration cooling
Porous
Conjugate gradient method
Two-dimensional

ABSTRACT

In this work, an inverse problem of the transient transpiration cooling is investigated in detail. The hot surface heat flux, which is dependent on time and space, is estimated according to the temperatures measured by thermal sensors. The local thermal non-equilibrium (LTNE) model is used to describe the energy conservation of transpiration cooling process and the thermal dispersion of coolant fluid in considered. The conjugate gradient method (CGM) is applied to solve this inverse problem. The accuracy of the inverse solutions is examined by a certain heat flux with given measurement errors. The examination shows that the inverse method presented by this work can obtain satisfactory results. The effect of variable thermal properties on the inverse solutions cannot be neglected since the large temperature gradient close to the hot surface. The suitable measurement times and points should be chose by considering acceptable accuracy, computational time and memory. Meanwhile, it is found out that the location should be close to the hot surface for more accuracy.

1. Introduction

Transpiration cooling has been proven as an effective mechanism of heat dissipation by a lot of investigators. In the investigations of [1–7], the cooling effectiveness on the hot surface exposed to a high heat flux, the thermal boundary conditions, the temperature distribution within porous matrix and the temperature gradient near the surface were discussed under the conditions of the heat flux given previously on the hot surface. But in actual fact, it is very important to determine the heat flux for the transpiration cooling control and ablation prevention. Glass et al. [8] numerically analyzed the convection and transpiration cooling effect on the surface exposed to a high temperature combustor using a boundary layer code and a porous media finite difference code, and solved the heat flux from the combustor with thermal boundary layer. Haeseler et al. [9] investigated transpiration cooled hydrogen–oxygen subscale chamber through experiments and computations, in order to establish the reference heat flux profile of the chamber, the pressures and temperatures at the inlet and outlet of the chamber were measured. In a practical transpiration cooling process, the heat flux on hot surface is dependent on space, operation state and coolant injection conditions, and it is a typical kind of inverse problems of heat transfer to determine the heat flux.

In recent years, the inverse problems have been discussed by many investigators. Huang and Huang [10] determined simultaneously the spatial-dependent effective thermal conductivity and volumetric heat capacity of a biological tissue based on temperature measurements. Hong and Baek [11] estimated the unsteady inlet temperature distribution for the two-phase laminar flow in a channel by downstream temperature measurements. Huang and Ozisik [12] calculated the spatial-dependent wall heat flux for the laminar flow in a parallel plate duct through temperature measurements. Li and Yan [13] solved an inverse problem for the unsteady convection in an annular duct, and used temperature data to determine the time and space dependent heat flux distribution on the inner wall of the duct. Chen et al. [14] calculated the time and space dependent heat transfer rate on the external wall of a pipe system with temperature measurements. Lin et al. [15] investigated the heat transfer flux of the unsteady laminar forced convection in parallel plate channels by temperature measurements. Li and Yang [16] used genetic algorithm (GA) in inverse radiation analysis for estimating the scattering albedo, optical thickness and phase function in parallel plane. Kim et al. [17] estimated wall emissivities by using hybrid genetic algorithm. Lee et al. [18] using repulsive particle swarm optimization method for estimating the unknown radiative parameters. Lee et al. [19] utilized the Karhunen–Loeve Galerkin procedure in the determination of the space-dependent wall heat flux for laminar flow inside a duct from the temperature measurement within the flow. However, these investigations were not aimed at the heat transfer within porous media or transpiration cooling, and in the references of [11–15], the assumptions of constant thermal properties and incompress-

* Corresponding author. Tel.: +86 551 3600945.
E-mail address: shijx@mail.ustc.edu.cn (J. Shi).

1290-0729/$ – see front matter
doi:10.1016/j.ijthermalsci.2008.11.019

Nomenclature

x, y	coordinate	St	Stanton number
X, Y	dimensionless coordinate	Bi	Biot number
H	thickness of entire structure ..... m	*Greek symbols*	
L	width of entire structure ..... m	ε	porosity
T	temperature ..... K	θ	dimensionless temperature
Z	dimensionless simulated temperature data	*Subscripts*	
k	thermal conductivity ..... W/m K	s	solid
h_{sf}	volumetric convective coefficient ..... W/m^2 K	f	fluid
α_{sf}	specific surface area ..... m^{-1}	c	coolant reservoir
h	interfacial convective coefficient ..... W/m^2 K	a	ablation
$\dot{m}$	coolant mass flow rate ..... kg/m^2 s	0	initial
M	dimensionless coolant flow rate	e	effective
c	specific heat capacity ..... J/kg K	ref	reference
q	hot surface heat flux ..... W/m^2	d	dispersion
Q	dimensionless heat flux		

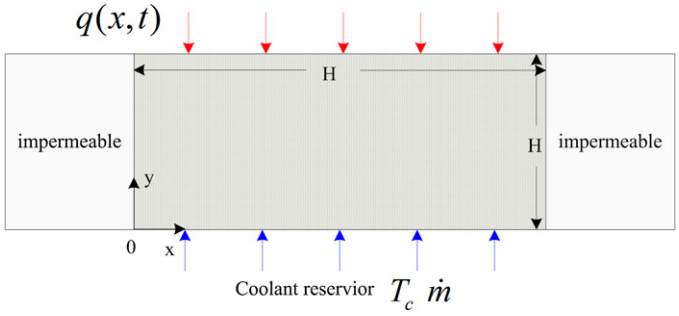

Fig. 1. Model of transpiration cooling.

ible fluid were used. It is clear that these assumptions may not be suitable for transpiration cooling, because there is a very large temperature gradient near the hot surface.

The inverse problem of the hot boundary is an important factor in the investigation on transpiration cooling, and the solution method of this problem is different from that of the normally inverse problem as mentioned above [10–19], because it concerns two coupled energy balance equations, flowing fluid and solid matrix. This paper presents a solution of the inverse problems with simulated temperature data. The aim is to provide the investigators with a relatively comprehensive conception to understand the hot boundary performance.

2. Direct model

In this work, the physical model of transpiration cooling is sketched in Fig. 1. Fluid coolant is injected into a porous matrix with a mass flow rate of $\dot{m}$ at a reservoir temperature of T_c to protect hot surface of the matrix from severe heat flux of q. In this paper, incompressible fluid and one-dimensional flow along y are assumed, and two-dimensional local thermal non-equilibrium models are utilized. The thermal diffusion and dispersion of coolant fluid are considered for more accurate estimation. The transient energy formulations are written as:

$$\begin{cases} (\rho c)_{f,e}\dfrac{\partial T_f}{\partial t} + (\rho c v)_f \dfrac{\partial T_f}{\partial y} \\ \quad = \dfrac{\partial}{\partial x}\left(k_{f,e}\dfrac{\partial T_f}{\partial x}\right) + \dfrac{\partial}{\partial y}\left(k_{f,e}\dfrac{\partial T_f}{\partial y}\right) + h_{sf}a_{sf}(T_s - T_f) \\ (\rho c)_{s,e}\dfrac{\partial T_s}{\partial t} = \dfrac{\partial}{\partial x}\left(k_{s,e}\dfrac{\partial T_s}{\partial x}\right) + \dfrac{\partial}{\partial y}\left(k_{s,e}\dfrac{\partial T_s}{\partial y}\right) - h_{sf}a_{sf}(T_s - T_f) \end{cases} \quad (1)$$

Here, k_e is the effective thermal conductivity: $k_{s,e} = (1-\varepsilon)k_s$, $k_{f,e} = \varepsilon k_f + k_d$. k_d is the thermal dispersion coefficient [20]:

$$k_{d,x} = 0.1Pr\left(\frac{\rho_f v d_p}{\mu}\right)k_f, \qquad k_{d,y} = 0.5Pr\left(\frac{\rho_f v d_p}{\mu}\right)k_f$$

$(\rho c)_e$ is the effective thermal capacity:

$$(\rho c)_{f,e} = \varepsilon(\rho c)_f, \qquad (\rho c)_{s,e} = (1-\varepsilon)(\rho c)_s$$

Initial condition:

$$t = 0,\ x \in [0, L],\ y \in [0, H], \quad T_s = T_f = T_0 \quad (2)$$

Here, initial temperature T_0 is same as the initial coolant temperature T_c.

To solve the governing equations, four boundary conditions are necessary. Wang and Shi [7] analyzed rationally five types of boundary conditions by analytical solution of the LTNE model. Considering their analysis and conclusion, the following equations can be suggested as boundary conditions:

$$t > 0, \quad y = 0 \begin{cases} h(T_s - T_c) = k_{e,s}\dfrac{\partial T_s}{\partial y} + k_{e,f}\dfrac{\partial T_f}{\partial y} \\ h(T_s - T_c) = \dot{m}c_f(T_f - T_c) \end{cases} \quad (3)$$

$$t > 0, \quad y = H \begin{cases} k_{e,s}\dfrac{\partial T_s}{\partial y}\Big|_{y=H} = q \\ \dfrac{\partial T_f}{\partial y}\Big|_{y=H} = 0 \end{cases} \quad (4)$$

$$t > 0, \quad x = 0 \frac{\partial T_s}{\partial x} = \frac{\partial T_f}{\partial x} = 0 \quad (5)$$

$$t > 0, \quad x = L \frac{\partial T_s}{\partial x} = \frac{\partial T_f}{\partial x} = 0 \quad (6)$$

Introduce the following dimensionless variables:

$$Y = \frac{y}{H}, \qquad X = \frac{x}{H}, \qquad T_{\text{ref}} = T_a - T_c$$
$$\theta = \frac{T - T_c}{T_{\text{ref}}}, \qquad M = \frac{H\dot{m}_f c_{f,\text{ref}}}{\varepsilon k_{f,\text{ref}}} \quad (7)$$

$$Q = \frac{qH}{(1-\varepsilon)k_{s,\text{ref}}T_{\text{ref}}}, \qquad Bi = \frac{h_{sf}a_{sf}H^2}{(1-\varepsilon)k_{s,\text{ref}}}$$
$$St_c = \frac{h_c}{(\rho v c)_{f,\text{ref}}} \quad (8)$$

T_c is the temperature of coolant in the reservoir and T_a is the ablation temperature of the porous matrix which the temperature

of hot surface cannot exceed. Accordingly, the dimensionless temperatures of solid and fluid only vary between 0 and 1. All the reference properties are taken at the initial temperature of T_0. The dimensionless formulations are rewritten as:

$$\frac{\partial\theta_f}{\partial\tau}+M\frac{(k/\rho c)_{f,\mathrm{ref}}}{(k/\rho c)_{s,\mathrm{ref}}}\frac{\partial\theta_f}{\partial Y}=\frac{(\rho c)_{s,\mathrm{ref}}}{(\rho c)_{f,e}}\frac{\partial}{\partial X}\left(\frac{k_{f,e}}{k_{s,\mathrm{ref}}}\frac{\partial\theta_f}{\partial X}\right)+\frac{(\rho c)_{s,\mathrm{ref}}}{(\rho c)_{f,e}}\frac{\partial}{\partial Y}\left(\frac{k_{f,e}}{k_{s,\mathrm{ref}}}\frac{\partial\theta_f}{\partial Y}\right)+Bi\frac{(\rho c)_{s,e,\mathrm{ref}}}{(\rho c)_{f,e}}(\theta_s-\theta_f) \tag{9}$$

$$\frac{\partial\theta_s}{\partial\tau}=\frac{(\rho c)_{s,\mathrm{ref}}}{(\rho c)_s}\frac{\partial}{\partial X}\left(\frac{k_s}{k_{s,\mathrm{ref}}}\frac{\partial\theta_s}{\partial X}\right)+\frac{(\rho c)_{s,\mathrm{ref}}}{(\rho c)_s}\frac{\partial}{\partial Y}\left(\frac{k_s}{k_{s,\mathrm{ref}}}\frac{\partial\theta_s}{\partial Y}\right)-Bi\frac{(\rho c)_{s,\mathrm{ref}}}{(\rho c)_s}(\theta_s-\theta_f) \tag{10}$$

$$\tau=0,\ X\in\left[0,\frac{L}{H}\right],\ Y\in[0,1],\quad \theta_s=\theta_f=\theta_0 \tag{11}$$

$$Y=0,\quad \begin{cases}\theta_f=St_c\theta_s\\ St_cM\dfrac{k_{f,e,\mathrm{ref}}}{k_{s,e}}\theta_s=\dfrac{\partial\theta_s}{\partial Y}+\dfrac{k_{f,e}}{k_{s,e}}\dfrac{\partial\theta_f}{\partial Y}\end{cases} \tag{12}$$

$$Y=1,\quad \begin{cases}\dfrac{k_s}{k_{s,\mathrm{ref}}}\dfrac{\partial\theta_s}{\partial Y}=Q\\ \dfrac{\partial\theta_f}{\partial Y}=0\end{cases} \tag{13}$$

$$X=0,\quad \frac{\partial\theta_s}{\partial X}=\frac{\partial\theta_f}{\partial X}=0 \tag{14}$$

$$X=\frac{L}{H},\quad \frac{\partial\theta_s}{\partial X}=\frac{\partial\theta_f}{\partial X}=0 \tag{15}$$

The direct problem (9)–(10) will be solved by finite difference method. It must be noted that when the thermal properties of coolant fluid and porous solid as thermal conductivity, capacity are variable and only temperature dependent, the coefficients in the non-linear equations and boundary conditions should be recalculated in each iterative step.

3. Conjugate gradient method for inverse problem

In the direct problem of transpiration cooling, the temperature distribution of coolant fluid and porous solid in the porous matrix is determined by the thermal properties, mass flow rate, initial and boundary conditions. In the inverse problem, the variation of temperature of coolant or porous is assumed to be measured inside the porous matrix or on the hot surface. The dimensionless heat flux on the hot surface $Q(X,\tau)$ is predicted by the measured temperature data. The solution of surface heat flux can be obtained by minimizing the object function as below:

$$J=\sum_{i=1}^{N}\sum_{j=1}^{M}(\theta_{i,j}-Z_{i,j})^2 \tag{16}$$

Here, $\theta(Y,X_i,\tau_j)$ is the computed dimensionless temperature with an estimated $Q(Y,X_i,\tau_j)$, $Z_i(Y,X_i,\tau_j)$ is the measured dimensionless temperature. i is the number of the measurement point along the X direction, N is the total number of the thermal couples embedded in the porous material. j is the number of the measurement interval in the τ direction, M is the total number of measurement times in a given period of time. If $Y=0$, the measurements are taken at the coolant surface. If $Y=1$, the measurements are taken at the hot surface. If $0<Y<1$, the measurements are taken in the porous matrix.

The inverse problem is ill-posed, and the estimated result of the heat flux is very sensitive to the measurement errors. That means they might not have unique solution. However there are many applications of inverse problem in engineering. To obtain a stable solution, different mathematical methods, Conjugate Gradient Method (CGM) [11–15], Genetic Algorithm (GA) [16,17], Particle Swarm Optimization (PSO) [18] and Karhunen–Loeve Galerkin Procedure (KLGP) [19] have been developed. The CGM is a quickly convergent algorithm in these methods [14,18], therefore it is applied in this work. The heat flux can be approximated by the following iterative process:

$$Q_{m,n}^{p+1}=Q_{m,n}^{p}-\beta^p d_{m,n}^{p} \tag{17}$$

Here $Q_{m,n}=Q(X_m,\tau_n)$, β^p is the step size, $d_{m,n}^{p}$ is the direction of descent given by

$$d_{m,n}^{p}=\left(\frac{\partial J}{\partial Q_{m,n}}\right)^p+\gamma^p d_{m,n}^{p-1} \tag{18}$$

Here, $(\partial J/\partial Q_{m,n})^p$ is the gradient of object function as:

$$\frac{\partial J}{\partial Q_{m,n}}=2\sum_{j=1}^{M}\sum_{i=1}^{N}(\theta_{i,j}-Z_{i,j})\frac{\partial\theta_{i,j}}{\partial Q_{m,n}} \tag{19}$$

Here, $d_{m,n}^{p-1}$ is the direction of descent at iteration $p-1$, γ^p is the conjugate coefficient which is calculated from

$$\gamma^p=\frac{\sum_{m=1}^{M}\sum_{n=1}^{N}\left[\left(\frac{\partial J}{\partial Q_{m,n}}\right)^p\right]^2}{\sum_{m=1}^{M}\sum_{n=1}^{N}\left[\left(\frac{\partial J}{\partial Q_{m,n}}\right)^{p-1}\right]^2},\quad \gamma^0=0 \tag{20}$$

The step size β^p is determined from

$$\beta^p=\frac{\sum_{j=1}^{M}\sum_{i=1}^{N}\left\{(\theta_{i,j}^{p}-Z_{i,j})\sum_{j=1}^{M}\sum_{i=1}^{N}\left(\frac{\partial\theta_{i,j}}{\partial Q_{m,n}}\right)^p d_{m,n}^{p}\right\}}{\sum_{j=1}^{M}\sum_{i=1}^{N}\left\{\sum_{m=1}^{M}\sum_{n=1}^{N}\left(\frac{\partial\theta_{i,j}}{\partial Q_{m,n}}\right)^p d_{m,n}^{p}\right\}^2} \tag{21}$$

Here, $\partial\theta_{i,j}/\partial Q_{m,n}$ is the sensitivity coefficient which can be calculated from the energy formulation by differentiating respect to $Q_{m,n}$. Considering the temperature dependent thermal properties, the differentiations of thermal properties respect to $Q_{m,n}$ must be included. The sensitivity coefficient equations and boundary conditions are expressed as:

$$\begin{aligned}&\frac{\partial(\rho c)_{f,e}}{(\rho c)_{f,e}\partial\theta_f}\frac{\partial\theta_f}{\partial Q_{m,n}}\frac{\partial\theta_f}{\partial\tau}+\frac{\partial}{\partial\tau}\left(\frac{\partial\theta_f}{\partial Q_{m,n}}\right)+M\frac{(k/\rho c)_{f,\mathrm{ref}}}{(k/\rho c)_{s,\mathrm{ref}}}\frac{\partial(\rho c)_{f,e}}{(\rho c)_{f,e}\partial\theta_f}\frac{\partial\theta_f}{\partial Q_{m,n}}\frac{\partial\theta_f}{\partial Y}+M\frac{(k/\rho c)_{f,\mathrm{ref}}}{(k/\rho c)_{s,\mathrm{ref}}}\frac{\partial}{\partial Y}\left(\frac{\partial\theta_f}{\partial Q_{m,n}}\right)\\&=\frac{(\rho c)_{s,\mathrm{ref}}}{(\rho c)_{f,e}}\frac{\partial}{\partial X}\left(\frac{1}{k_{s,\mathrm{ref}}}\left(\frac{\partial k_{f,e}}{\partial\theta_f}\frac{\partial\theta_f}{\partial Q_{m,n}}\frac{\partial\theta_f}{\partial X}+k_{f,e}\frac{\partial}{\partial X}\left(\frac{\partial\theta_f}{\partial Q_{m,n}}\right)\right)\right)+\frac{(\rho c)_{s,\mathrm{ref}}}{(\rho c)_{f,e}}\frac{\partial}{\partial Y}\left(\frac{1}{k_{s,\mathrm{ref}}}\left(\frac{\partial k_{f,e}}{\partial\theta_f}\frac{\partial\theta_f}{\partial Q_{m,n}}\frac{\partial\theta_f}{\partial Y}+k_{f,e}\frac{\partial}{\partial Y}\left(\frac{\partial\theta_f}{\partial Q_{m,n}}\right)\right)\right)\\&\quad+Bi\frac{(\rho c)_{s,e,\mathrm{ref}}}{(\rho c)_{f,e}}\left(\frac{\partial\theta_s}{\partial Q_{m,n}}-\frac{\partial\theta_f}{\partial Q_{m,n}}\right)\end{aligned} \tag{22}$$

$$\begin{aligned}&\frac{\partial(\rho c)_s}{(\rho c)_s\partial\theta_s}\frac{\partial\theta_s}{\partial Q_{m,n}}\frac{\partial\theta_s}{\partial\tau}+\frac{\partial}{\partial\tau}\left(\frac{\partial\theta_s}{\partial Q_{m,n}}\right)\\&=\frac{(\rho c)_{s,\mathrm{ref}}}{(\rho c)_s}\frac{\partial}{\partial X}\left(\frac{1}{k_{s,\mathrm{ref}}}\left(\frac{\partial k_s}{\partial\theta_s}\frac{\partial\theta_s}{\partial Q_{m,n}}\frac{\partial\theta_s}{\partial X}+k_s\frac{\partial}{\partial X}\left(\frac{\partial\theta_s}{\partial Q_{m,n}}\right)\right)\right)+\frac{(\rho c)_{s,\mathrm{ref}}}{(\rho c)_s}\frac{\partial}{\partial Y}\left(\frac{1}{k_{s,\mathrm{ref}}}\left(\frac{\partial k_s}{\partial\theta_s}\frac{\partial\theta_s}{\partial Q_{m,n}}\frac{\partial\theta_s}{\partial Y}+k_s\frac{\partial}{\partial Y}\left(\frac{\partial\theta_s}{\partial Q_{m,n}}\right)\right)\right)\\&\quad-Bi\frac{(\rho c)_{s,\mathrm{ref}}}{(\rho c)_s}\left(\frac{\partial\theta_s}{\partial Q_{m,n}}-\frac{\partial\theta_f}{\partial Q_{m,n}}\right)\end{aligned} \tag{23}$$

$$\tau = 0, Y \in [0,1]$$
$$\frac{\partial \theta_s(Y)}{\partial Q_{m,n}} = \frac{\partial \theta_f(Y)}{\partial Q_{m,n}} = 0 \tag{24}$$

$$\tau > 0, Y = 0$$
$$\begin{cases} St_c M \dfrac{k_{f,e,\mathrm{ref}}}{k_{s,e}} \left(\dfrac{\partial \theta_s}{\partial Q_{m,n}} \right) \\ \quad = \dfrac{\partial k_{s,e}}{k_{s,e} \partial \theta_s} \dfrac{\partial \theta_s}{\partial Q_{m,n}} \dfrac{\partial \theta_s}{\partial Y} + \dfrac{\partial}{\partial Y} \left(\dfrac{\partial \theta_s}{\partial Q_{m,n}} \right) \\ \qquad + \dfrac{\partial k_{f,e}}{k_{s,e} \partial \theta_f} \dfrac{\partial \theta_f}{\partial Q_{m,n}} \dfrac{\partial \theta_f}{\partial Y} + \dfrac{k_{f,e}}{k_{s,e}} \dfrac{\partial}{\partial Y} \left(\dfrac{\partial \theta_f}{\partial Q_{m,n}} \right) \\ \dfrac{\partial \theta_f}{\partial Q_{m,n}} = St_c \dfrac{\partial \theta_s}{\partial Q_{m,n}} \end{cases} \tag{25}$$

$$\tau > 0, Y = 1$$
$$\begin{cases} \dfrac{1}{k_{s,\mathrm{ref}}} \left(k_s \dfrac{\partial}{\partial Y} \left(\dfrac{\partial \theta_s}{\partial Q_{m,n}} \right) + \dfrac{\partial k_s}{\partial \theta_s} \dfrac{\partial \theta_s}{\partial Q_{m,n}} \dfrac{\partial \theta_s}{\partial Y} \right) \\ \quad = \hat{u}(X - X_m, \tau - \tau_n) \\ \dfrac{\partial}{\partial Y} \left(\dfrac{\partial \theta_f}{\partial Q_{m,n}} \right) = 0 \end{cases} \tag{26}$$

$$\tau > 0, X = 0$$
$$\frac{\partial}{\partial X} \left(\frac{\partial \theta_s}{\partial Q_{m,n}} \right) = \frac{\partial}{\partial X} \left(\frac{\partial \theta_f}{\partial Q_{m,n}} \right) = 0 \tag{27}$$

$$\tau > 0$$
$$X = \frac{L}{H} \frac{\partial}{\partial X} \left(\frac{\partial \theta_s}{\partial Q_{m,n}} \right) = \frac{\partial}{\partial X} \left(\frac{\partial \theta_f}{\partial Q_{m,n}} \right) = 0 \tag{28}$$

Here,

$$\hat{u}(X - X_m, \tau - \tau_n) = \begin{cases} 1 & \text{if } X = X_m \text{ and } \tau = \tau_n \\ 0 & \text{otherwise} \end{cases} \tag{29}$$

When the thermal properties are constant, the values of $\partial(\rho c)_{f,e}/\partial\theta_f$, $\partial(\rho c)_s/\partial\theta_s$, $\partial k_{f,e}/\partial\theta_f$, $\partial k_s/\partial\theta_s$ and $\partial k_{s,e}/\partial\theta_s$ would be zero, Eqs. (22)–(23) can be solved by using the finite difference approach referred to direct problem (9)–(10) previously.

When the thermal properties are variable, the non-linear equations (22)–(23) are more complicated than Eqs. (9)–(10). It is noticed that the values of $\partial\theta_i/\partial\tau$, $\partial\theta_i/\partial X$ and $\partial\theta_i/\partial Y$ $(i = s, f)$ have been known in previous calculation step, simultaneously, the values of $\partial(\rho c)_{f,e}/\partial\theta_f$, $\partial k_{f,e}/\partial\theta_f$, $\partial k_s/\partial\theta_s$ and $\partial k_{s,e}/\partial\theta_s$ can be calculated through the formulations given below. The non-linear equations (22)–(23) also can be solved with the finite difference approach. Accordingly, the coefficients in the sensitivity coefficient equations and boundary conditions will vary with time when the thermal properties are temperature dependent. Then the sensitivity $\partial\theta/\partial Q_{m,n}$ must be recalculated in each measure time step under this condition.

If the inverse problem contains no measurement errors, the iteration stopping criterion is $J < \sigma, \sigma$ is a small specific positive number, in this paper, it take as 10^{-5}.

However, the measurement data do contain random error with a standard deviation η, and then the stopping criterion is modified as

$$J < NM\eta^2 \tag{30}$$

The computational procedure for the inverse problem of transpiration cooling is expressed as follows:

Step 1. Given an guess heat flux $Q^0_{m,n} = 0$. Solve the energy equations (9)–(10) for the temperature $\theta_{i,j}$.

Step 2. Calculate the objective function J(16). If the stopping criterion is satisfied the iteration procedure terminates. Otherwise go to step 3.

Step 3. Solve the sensitivity equations (22)–(23) for the sensitivity coefficient $\partial\theta_{i,j}/\partial Q_{m,n}$.

Step 4. According $\partial\theta_{i,j}/\partial Q_{m,n}$, $\theta_{i,j}$ and $Z_{i,j}$, compute $\partial J/\partial Q_{m,n}$ (19), γ^p (20), $d^p_{m,n}$ (18) and β^p (21).

Step 5. According $d^p_{m,n}$ and β^p, compute $Q^{p+1}_{m,n}$ (17), set $p = p + 1$ and go to step 2.

4. Results and discussion

The accuracy of the present inverse method for the estimation of the heat flux without prior information is illustrated by using two kinds of heat flux formulation. The effects of variable thermal properties, sensor location and measurement error on the results are discussed. The simulated measured temperature data Z are generated by adding random errors to the exact temperature data θ which are calculated from the solution of the given heat flux:

$$Z = \theta + \eta\xi \tag{31}$$

Where η is the standard deviation of the measurement temperature data, ξ is a random variable within (-2.576)–2.576 for 99% confidence bound.

In order not to affect the internal and external flow field, in this paper, the thermal sensors are assumed to be embedded in the porous solid. That means $\theta_{i,j}$ and $\partial\theta_{i,j}/\partial Q_{m,n}$ take as $\theta_{s,i,j}$ and $\partial\theta_{s,i,j}/\partial Q_{m,n}$ respectively.

Two kinds of time dependent heal flux on hot surface are written as below

$$\text{G1.} \quad Q(\tau) = 20\mathrm{abs}\left(\sin\left(\frac{\pi\tau}{0.18} + \frac{2\pi X}{L/H} \right) \right) \tag{32}$$

$$\text{G2.} \quad Q(\tau) = 10 + 10\cos\left(\frac{\pi\tau}{0.18} + \frac{2\pi X}{L/H} \right) \tag{33}$$

In this work, the thermal properties of the coolant fluid and porous solid are considered as only temperature dependent and taken as below:

$$k_s \ (\mathrm{W/m\,K}) = 7.86 + 1.73 \times 10^{-2} T - 1.50 \times 10^{-5} T^2 + 9.14 \times 10^{-9} T^3 \tag{34}$$

$$k_f \ (\mathrm{W/m\,K}) = 5.49 \times 10^{-2} \tag{35}$$

$$c_{ps} \ (\mathrm{J/kg\,K}) = 422.69 + 0.26T - 3.22 \times 10^{-4} T^2 + 1.92 \times 10^{-7} T^3 \tag{36}$$

$$c_{pf} \ (\mathrm{J/kg\,K}) = 1029.18 - 0.23T + 5.86 \times 10^{-4} T^2 - 2.45 \times 10^{-7} T^3 \tag{37}$$

$$\rho_s \ (\mathrm{kg/m^3}) = 7860, \quad T_a \ (\mathrm{K}) = 1250$$
$$T_c \ (\mathrm{K}) = T_0 \ (\mathrm{K}) = 293 \tag{38}$$

Other parameters in this paper are taken as below:

$$\varepsilon = 0.3, \quad Bi = 5.0\mathrm{E}3, \quad Stc = 1$$
$$Pr = 0.7, \quad M = 2.0\mathrm{E}2, \quad L/H = 2 \tag{39}$$

The measurements are taken at the hot surface by default. The comparison between the exact heat flux and the inverse solutions obtained with no measurement errors are shown in Fig. 2. It can be found from Fig. 2 that the inverse solutions are in well agreement with the exact results.

Fig. 3 shows the influence of the variation in thermal properties on the inverse solutions. The two heat fluxes of the inverse solutions obtained by constant thermal properties obviously underestimate the heat flux. These results are reasonable. If the thermal

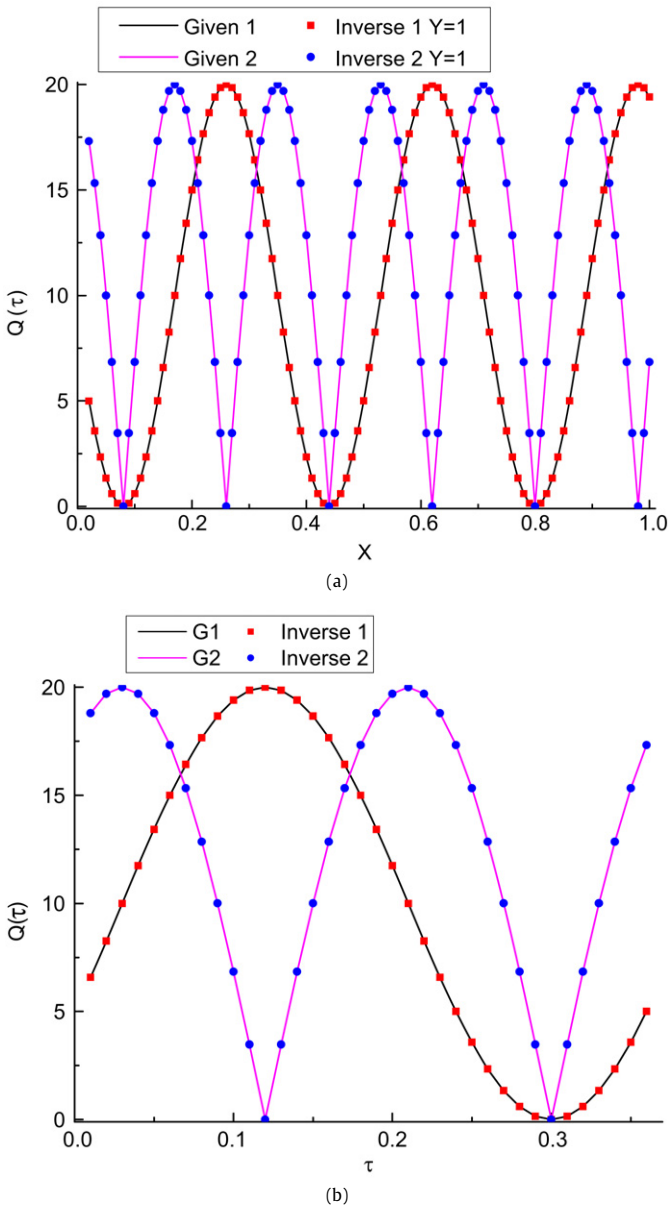

Fig. 2. Inverse solutions with two case heat flux formulation and no measure errors: (a) at $\tau = 0.1$, (b) at $X = 0.45$.

properties are mutative, they would increase as temperature raise according the relationship formulations. Therefore, under the same heat flux, the direct solutions with varied thermal properties can obtain lower temperature than that with constant thermal properties [2]. Correspondingly, the most underestimations take place under the highest heat flux. From these comparisons, it can be seen that the influences of the thermal properties on the inverse solution should be considered in the thermal system with large temperature gradient.

The comparison between the exact heat flux and the inverse solutions obtained with standard deviation $\eta = 0.5\%$ and $\eta = 1.0\%$ are shown in Figs. 4–5. It can be found from Figs. 4–5 that although the measurement errors are introduced, the inverse method in this work can also obtain the satisfactory solutions. Simultaneously, the worse accuracy appears at the peak value and bottom value of the heat flux.

To analyze the influence of the measurement times of N and the number of thermal couples of M on the inverse solutions, an

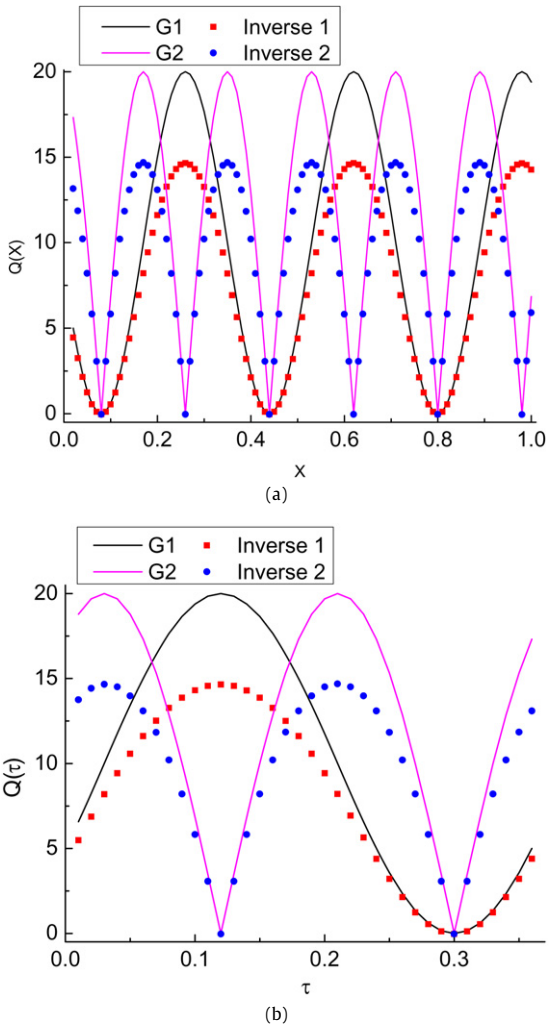

Fig. 3. Effect of variable thermal properties on the inverse solutions with no measure errors: (a) at $\tau = 0.1$, (b) at $X = 0.45$.

absolute average error in the estimated heat flux is defined as below:

$$f_{\mathrm{err}} = \frac{1}{NM}\sum_{j=1}^{M}\sum_{i=1}^{N}\left|Q_{i,j}^{g} - Q_{i,j}^{e}\right| \tag{40}$$

Here, $Q_{i,j}^{g}$ is the given heat flux G1, $Q_{i,j}^{e}$ is the heat flux obtained by the measured temperature with the given standard deviations 0.5%. Fig. 6 illustrates the influence of the measurement times and the number of thermal couples on the inverse solutions. N are taken as 50, 55, 60, 65, 70, 75, 80, 85, 90, 95, 100 respectively, and M are taken as 9, 18, 27, 36, 45, 54, 63, 72 respectively. It can be seen that average errors decrease observably with the increase in N from 50 to 75 and M from 9 to 54, but have no any significant change in N from 75 to 100 and M from 54 to 72. Simultaneously, some slightly rising variations take place, it is believed to be caused by increased computational errors.

It is known that the computational time and memory also increase under larger measure times and number of thermal couples. As a result, 100×36 measurement times and number of thermal couples for all of the solutions presented in this paper except in Fig. 6.

Fig. 7 illustrates the influence of measurement positions Y on the inverse solution. The standard deviation is 0.5%. It is clear that the positions more far away from the hot surface, the inverse solutions are far away from the given heat flux. The same conclusion

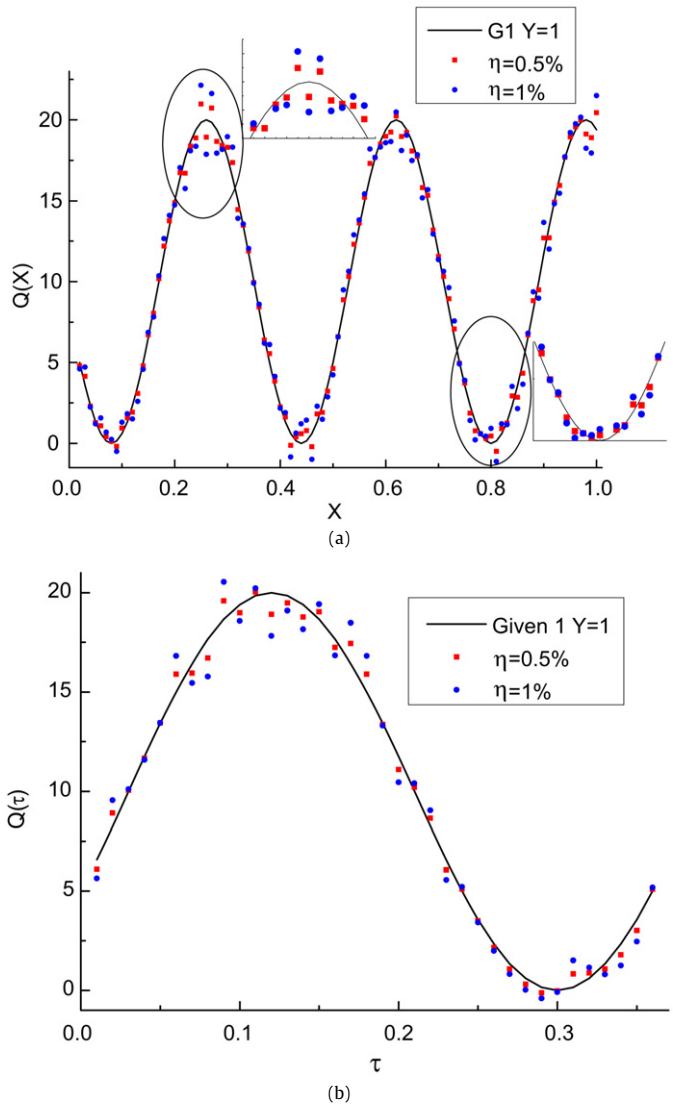

Fig. 4. Inverse solutions with given case 1 heat flux and standard deviation 0.5% and 1.0%: (a) at $\tau = 0.1$, (b) at $X = 0.45$.

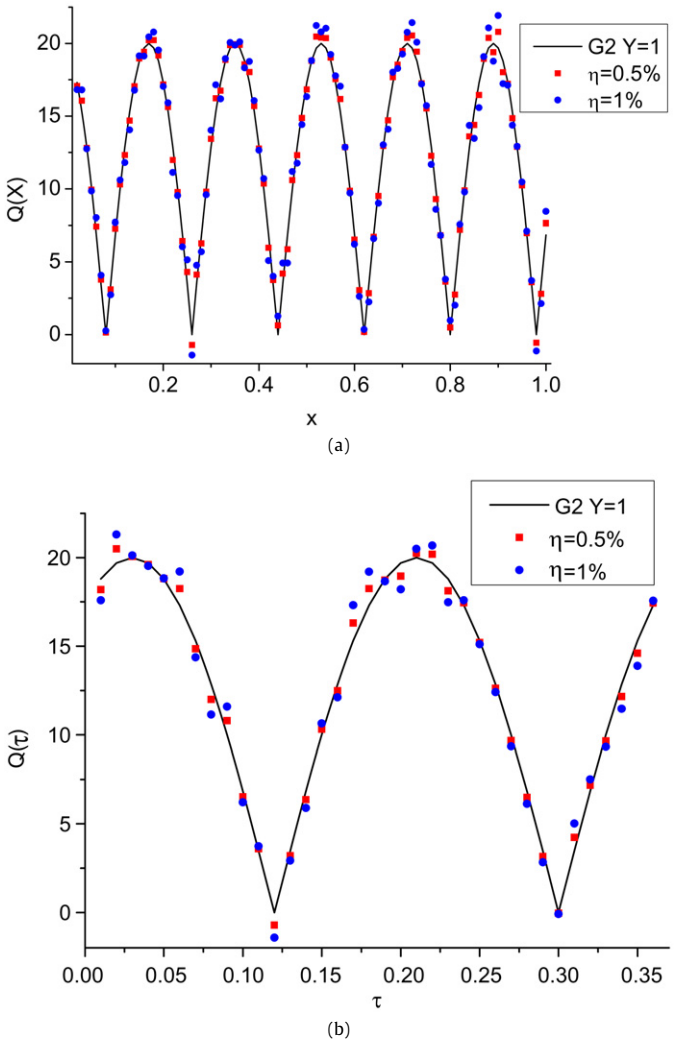

Fig. 5. Inverse solutions with given case 2 heat flux and standard deviation 0.5% and 1.0%: (a) at $\tau = 0.1$, (b) at $X = 0.45$.

was drawn by Lin [15]. The worse accuracy appears at the peak value and bottom value of the heat flux.

This phenomenon can be explained by Fig. 8. The solid temperature distributions within the matrix in Fig. 8 are obtained at one m. It can be observed that in the region from $Y = 0$ to 0.8, the variation of the solid temperatures are very small. For 0.8 to 1, the solid temperature increase quickly. Therefore, the more far away from the hot surface, the same absolute measurement errors will lead to a larger relative error.

5. Conclusion

An inverse method for estimating the time-dependent heat flux for transpiration cooling is presented in this work. The local thermal non-equilibrium model and conjugate gradient method are used to solve the inverse problem with the solid matrix temperature measured. Through this work, the following conclusions can be drawn:

- The inverse method for estimating the heat flux on the hot surface can be successfully applied to solve transpiration cooling problem.

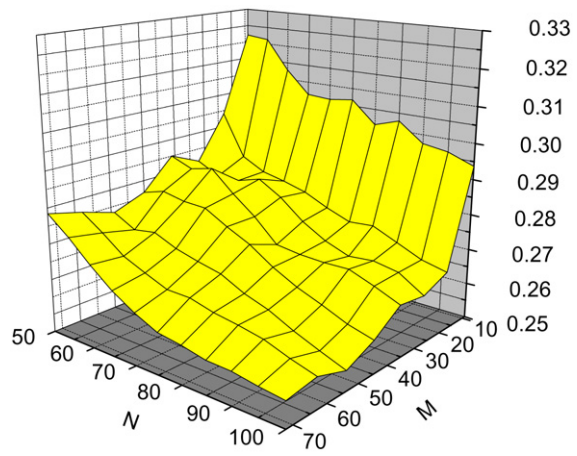

Fig. 6. Effects of measurement times and number of thermal couples on the inverse solutions.

- In the numerical calculation of the inverse problem, the variations in the thermal properties should be considered in the thermal system with large temperature gradient.
- Considering the computational time and memory, the suitable measurement times and points can be chose for acceptable accuracy.

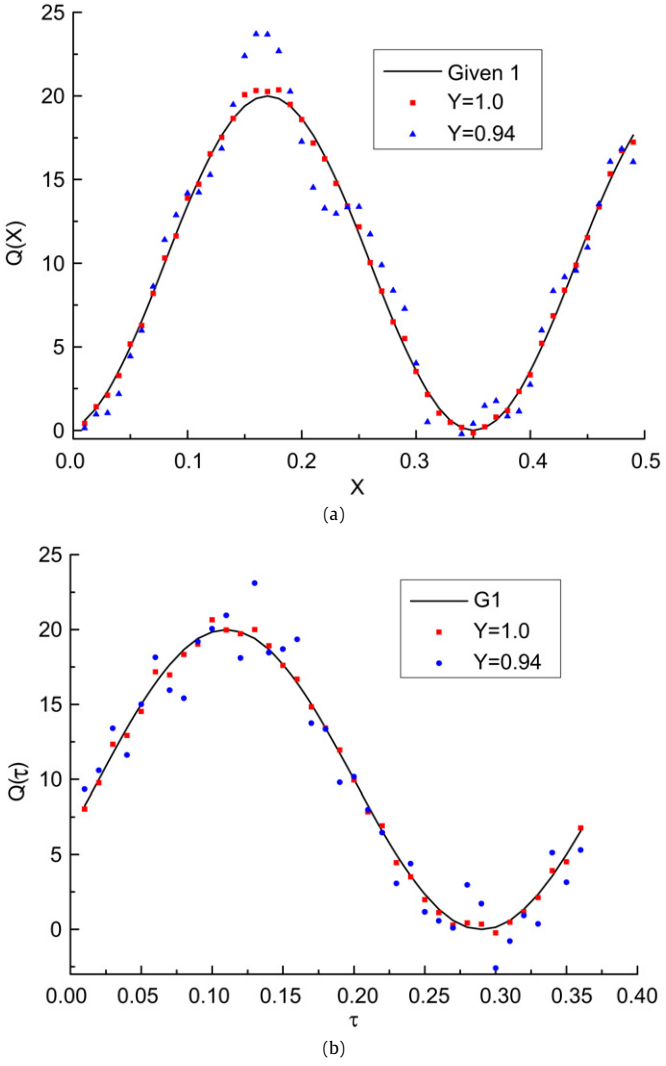

Fig. 7. Inverse solutions with three sensor position and standard deviation 0.5%: (a) at $\tau = 0.18$, (b) at $X = 0.25$.

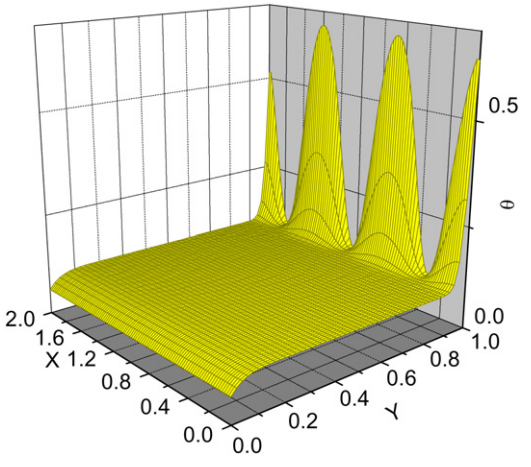

Fig. 8. Temperature distribution in porous matrix of transpiration cooling.

- As the input temperature of the inverse problem, the measurement point within the solid matrix should be close to the hot surface for better accuracy.

Acknowledgements

The project is supported by National Natural Science Foundation of China (No. 10772175) and (No. 90305006).

References

[1] J.A. Landis, J.W. Bowman, Numerical study of a transpiration cooled rocket nozzle, in: AIAA Meeting 1996, Paper 96-2580.
[2] H.N. Wang, J.H. Wang, A numerical investigation of ablation and transpiration cooling using the local thermal non-equilibrium model, in: Proceeding of the 42nd AIAA/ASME/SAE/ASEE Joint Propulsion Conference & Exhibit, Sacramento, California, July 9–12, 2006, AIAA-2006-5264.
[3] J.H. Wang, H.N. Wang, J.G. Sun, J. Wang, Numerical simulation of control ablation by transpiration cooling, Heat and Mass Transfer 43 (2007) 471–478.
[4] D. Greuel, A. Herbertz, O.J. Haidn, M. Ortelt, H. Hald, Transpiration cooling applied to C/C liners of cryogenic liquid rocket engines, AIAA 2004-3682.
[5] J.V. Wolfersdorf, Effect of coolant side heat transfer on transpiration cooling, Heat and Mass Transfer 41 (2005) 327–337.
[6] V.I. Kovenskii, Yu.S. Teplitskii, Modelling of heat transfer in an infiltrated granular bed in view of the difference of phase temperatures, International Journal of Heat and Mass Transfer 49 (2006) 359–365.
[7] J.H. Wang, J.X. Shi, A discussion of boundary conditions of transpiration cooling problems using analytical solution of LTNE model, ASME Journal of Heat Transfer 130 (2008) 014504-1–014504-5.
[8] D.E. Glass, A.D. Dilley, H.N. Kelly, Numerical analysis of convection transpiration cooling, NASA/TM-1999-209828.
[9] D. Haeseler, C. Mading, V. Rubinskiy, V. Gorokhov, S. Khrisanfov, Experimental investigation of transpiration cooled hydrogen–oxygen subscale chambers, AIAA-98-3364.
[10] C.-H. Huang, C.-Y. Huang, An inverse problem in estimating simultaneously the effective thermal conductivity and volumetric heat capacity of biological tissue, Applied Mathematical Modeling 31 (2007) 1785–1797.
[11] Y.K. Hong, S.W. Baek, Inverse analysis for estimating the unsteady inlet temperature distribution for two-phase laminar flow in a channel, International Journal of Heat and Mass Transfer 49 (2006) 1137–1147.
[12] Ch. Huang, Inverse problem of determining unknown wall heat-flux in laminar-flow through a parallel plate duct, Numerical Heat Transfer A 21 (1992) 55–70.
[13] H.-Y. Li, W.-M. Yan, Inverse convection problem for determining wall heat flux in annular duct flow, ASME Journal of Heat Transfer 122 (2000) 460–464.
[14] W.-L. Chen, Y.-C. Yang, W.-J. Chang, H.-L. Lee, Inverse problem of estimating transient heat transfer rate on external wall of forced convection pipe, Energy Conversion and Management 49 (2008) 2117–2123.
[15] D.T.W. Lin, W.M. Yan, H.Y. Li, Inverse problem of unsteady conjugated forced convection in parallel plate channels, International Journal of Heat and Mass Transfer 51 (2008) 993–1002.
[16] H.Y. Li, C.Y. Yang, A genetic algorithm for inverse radiation problems, International Journal of Heat and Mass Transfer 40 (1997) 1545–1549.
[17] K.W. Kim, S.W. Baek, M.Y. Kim, H.S. Ryu, Estimation of emissivities in a two-dimensional irregular geometry by inverse radiation analysis using hybrid genetic algorithm, Journal of Quantitative Spectroscopy and Radiative Transfer 87 (2004) 1–14.
[18] K.H. Lee, S.W. Baek, K.W. Kim, Inverse radiation analysis using repulsive particle swarm optimization algorithm, International Journal of Heat and Mass Transfer 51 (2008) 2772–2783.
[19] H.M. Park, J.H. Lee, A method of solving inverse convection problem by means of mode reduction, Chemical Engineering Science 53 (1998) 1731–1744.
[20] B. Alazmi, K. Vafai, Analysis of variants within the porous media transport models, ASME J. Heat Transfer 122 (2000) 303–326.